Article

Generating New FANCA-Deficient HNSCC Cell Lines by Genomic Editing Recapitulates the Cellular Phenotypes of Fanconi Anemia

Ricardo Errazquin [1,2], Esther Sieiro [2], Pilar Moreno [2], María José Ramirez [3,4], Corina Lorz [1,2,5], Jorge Peral [2], Jessica Ortiz [2], José Antonio Casado [4,6,7], Francisco J. Roman-Rodriguez [4,6,7], Helmut Hanenberg [8,9], Paula Río [4,6,7], Jordi Surralles [3,4], Carmen Segrelles [1,2,5] and Ramon Garcia-Escudero [1,2,5,*]

1   Biomedical Research Institute I+12, University Hospital 12 de Octubre, 28041 Madrid, Spain; Ricardo.ErrazquinCiudad@externos.ciemat.es (R.E.); clorz@ciemat.es (C.L.); carmen.segrelles@ciemat.es (C.S.)
2   Molecular Oncology Unit, CIEMAT, 28040 Madrid, Spain; esiba96@gmail.com (E.S.); pilar.msanc@gmail.com (P.M.); Jorge.Peral@ciemat.es (J.P.); jessica.ortiz@ciemat.es (J.O.)
3   Join Research Unit on Genomic Medicine UAB-Sant Pau Biomedical Research Institute, Hospital de la Santa Creu i Sant Pau, 08041 Barcelona, Spain; mariajose.ramirez@uab.cat (M.J.R.); jordi.surralles@uab.cat (J.S.)
4   Centro de Investigación Biomédica en Enfermedades Raras (CIBERER), 28029 Madrid, Spain; jose.casado@ciemat.es (J.A.C.); franjrr_@hotmail.com (F.J.R.-R.); paula.rio@ciemat.es (P.R.)
5   Centro de Investigación Biomédica en Red de Cáncer (CIBERONC), 28029 Madrid, Spain
6   Hematopoietic Innovative Therapies Division, CIEMAT, 28040 Madrid, Spain
7   Instituto de Investigaciones Sanitarias de la Fundación Jiménez Díaz, 28040 Madrid, Spain
8   University Children's Hospital Essen, University of Duisburg-Essen, 47057 Essen, Germany; helmut.hanenberg@uk-essen.de
9   Department of Otorhinolaryngology & Head/Neck Surgery, Heinrich Heine University, 40225 Düsseldorf, Germany
*   Correspondence: ramon.garcia@ciemat.es

Abstract: Fanconi anemia (FA) patients have an exacerbated risk of head and neck squamous cell carcinoma (HNSCC). Treatment is challenging as FA patients display enhanced toxicity to standard treatments, including radio/chemotherapy. Therefore, better therapies as well as new disease models are urgently needed. We have used CRISPR/Cas9 editing tools in order to interrupt the human *FANCA* gene by the generation of insertions/deletions (indels) in exon 4 in two cancer cell lines from sporadic HNSCC having no mutation in FA-genes: CAL27 and CAL33 cells. Our approach allowed efficient editing, subsequent purification of single-cell clones, and Sanger sequencing validation at the edited locus. Clones having frameshift indels in homozygosis did not express FANCA protein and were selected for further analysis. When compared with parental CAL27 and CAL33, *FANCA*-mutant cell clones displayed a FA-phenotype as they (i) are highly sensitive to DNA interstrand crosslink (ICL) agents such as mitomycin C (MMC) or cisplatin, (ii) do not monoubiquitinate FANCD2 upon MMC treatment and therefore (iii) do not form FANCD2 nuclear foci, and (iv) they display increased chromosome fragility and G2 arrest after diepoxybutane (DEB) treatment. These *FANCA*-mutant clones display similar growth rates as their parental cells. Interestingly, mutant cells acquire phenotypes associated with more aggressive disease, such as increased migration in wound healing assays. Therefore, CAL27 and CAL33 cells with *FANCA* mutations are phenocopies of FA-HNSCC cells.

Keywords: Fanconi anemia; CRISPR/Cas9; gene editing; FANCA; head and neck cancer

1. Introduction

Fanconi anemia (FA) is a rare DNA repair deficiency disorder characterized by hypersensitivity to DNA interstrand crosslink (ICL) agents and chromosome instability [1,2]. In most cases the disease is autosomal recessive, with the exception of *FANCB*, which is X-linked, and mutations in the oligomerization domain of RAD51/FANCR, which are

dominant negative. FA patients display varying degrees of developmental abnormalities, bone marrow failure (BMF), and increased cancer incidence. FA is due to functional inactivation of any one of 23 FA genes involved in DNA repair. The FA proteins together with FA-associated proteins interact in a pathway to repair ICL known as the FA pathway or the FA–BRCA pathway [2]. The pathway involves detection of the DNA crosslink at the stalled replication fork, unhooking of the crosslink, local generation of a double-strand break, and the use of homologous recombination (HR) proteins downstream to repair the break. The management of the BMF disease has remarkably improved over the last 20 years, predominantly due to improved outcome/survival of allogeneic hematologic stem cell transplantation, and more recently to hematopoietic gene therapy [3]. Therefore, FA patient survival has increased from less than 20 years of age in the 1990s to more than 30 years observed today [4,5]. However, one of the most challenging health issues in older/transplanted FA patients is appearance of solid tumors such as head and neck squamous cell cancer (HNSCC) relatively early in life. Although first chemoprevention studies with quercetin or metformin [6,7] are currently conducted, treatment options are limited to curative surgery and some radiotherapy, as most FA patients display high toxicities to treatment with DNA alkylating agents and especially platinum derivatives, which form the backbone of solid cancer therapy. Compared with non-FA patients, FA-HNSCC is diagnosed at much more advanced stages, and recurrence/metastatic disease is more frequent [8]. As a consequence, patient survival is very poor (25% at 5 years) [8] and therefore new therapeutic options are needed.

Discovery and preclinical testing of new cancer treatments for FA patients is also dependent on the availability of clinical specimens for basic research purposes, which are rather scarce in the case of rare diseases such as FA. As only a handful of HNSCC cell lines derived from FA patients exists worldwide, and the characteristics of the cell lines including the genetic information and the sensitivity profiles to anticancer compounds are largely unknown [9–11], we propose in this report to use genetic engineering on well-established HNSCC cell lines in order to generate new FA-deficient cell line models for studying FA-HNSCC. The main advantages of using such engineered FA cell lines are that their molecular aberrations [12,13] and sensitivity profiles to many compounds have already been determined [14] and in vivo xenograft models established [15]. To this end, biallelic inactivation of *FANCA*, the gene most frequently mutated in FA patients (60%), was achieved by CRISPR/Cas9 editing of CAL27 and CAL33 non-FA, two well-known oral cancer cell lines. The results presented here showed that edited clones display all FA-associated phenotypes, validating them as reliable FA-HNSCC models.

2. Results

2.1. Biallelic Mutation in the FANCA Gene by CRISPR/Cas9 Editing in Non-FA HNSCC Cell Lines

Most HNSCC in FA patients are localized in the oral cavity, mainly in the tongue. Therefore, we selected oral cancer cell lines from non-FA patients having no mutations in any of the 23 FA genes. Therefore, we mined into the CCLE data in the cBioPortal (https://www.cbioportal.org, accessed on 1 September 2020) and selected CAL27 and CAL33 cells, which display mean levels of the *FANCA* mRNA when compared with similar cell lines, and no amplification into the *FANCA* locus (Figure S1 and Table S1). CAL27 and CAL33 cells were nucleofected with a ribonucleoprotein complex constituted by the CRISPR guide RNA (gRNA) gGM10 targeting *FANCA* gene and purified Cas9 protein (see Materials and Methods) (Figure 1A). Nucleofection conditions were set up to favor non-homologous end joining (NHEJ) repair after DNA excision by the gRNA/Cas9 complex. Before single cells were cloned and expanded, an estimation of editing efficiency was performed using a nuclease assay and specific primers (Table S2). Sanger sequencing was performed on selected clones to assess for inactivating mutations in both alleles. A high proportion (>90%) of sequenced clones from both CAL27 and CAL33 displayed *FANCA* gene editing (Figure 1B). Knock-out score (KO-score) was estimated for each clone upon Sanger sequencing using the ICE algorithm [16] (Figure 1C). Four clones of each parental

cell line having highest KO-scores displayed negligible levels of FANCA protein, validating the editing approach (Figure 1D). Two of these clones were selected for further analyses: clones c34 and c47 for CAL27, and clones c5 and c11 for CAL33. The edited sequences at the *FANCA* locus in each of these four clones are shown in Figures S2 and S3.
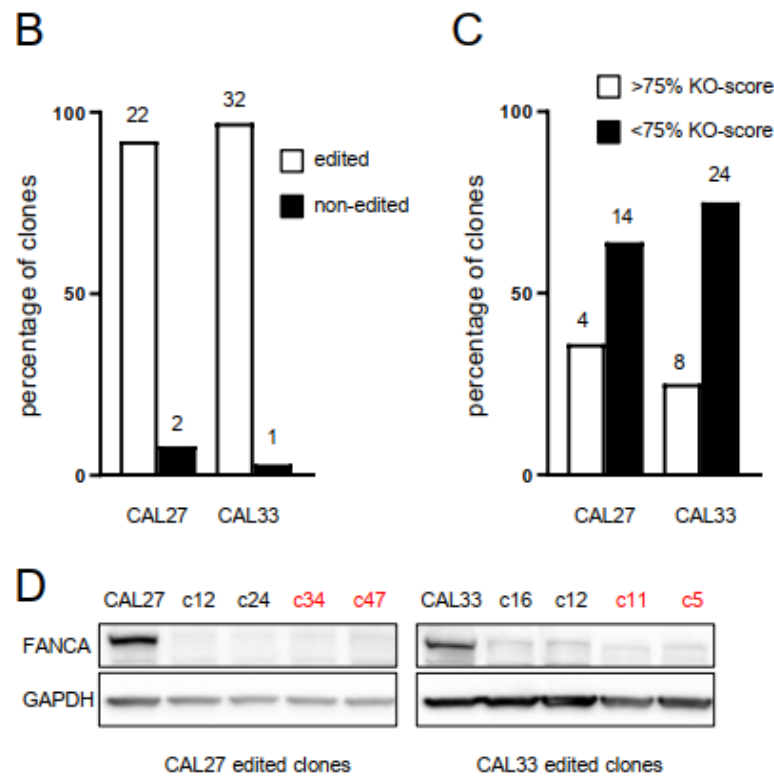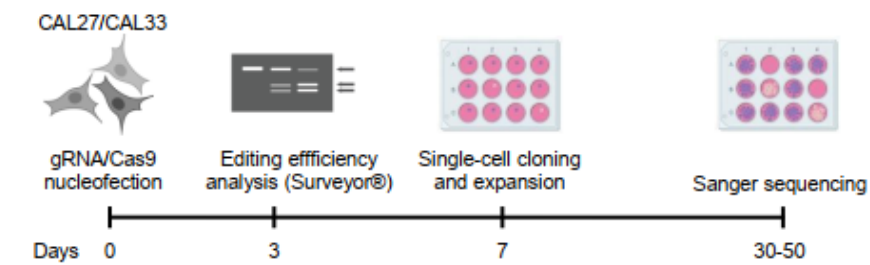

Figure 1. Biallelic mutation in *FANCA* gene by CRISPR/Cas9 editing in non-FA HNSCC cell lines. (**A**) Schematic model of *FANCA*-mutant clones generation. CAL27 and CAL33 cells were nucleofected with a ribonucleoprotein mix of a *FANCA* gene CRISPR guide RNA (gRNA) and purified Cas9 protein. Editing efficiency was evaluated three days after by nuclease assay using the Surveyor® Mutation Detection Kit (IDT). Single cells were plated using fluorescence-activated cell sorting (FACS) and expanded in conditioned medium. Sanger sequencing was performed on randomly selected, single-cell clones to assess for inactivating mutations in both alleles. (**B**) The vast majority of sequenced clones displayed *FANCA*-gene editing, both from CAL27 and CAL33 cells. Numbers of edited or non-edited clones are shown above each bar. (**C**) Knock-out score (KO-score) was estimated for each clone upon Sanger sequencing using the ICE algorithm [16]. Between 24% and 36% of edited clones displayed high KO scores (>75%). (**D**) Clones having highest KO scores display negligible levels of FANCA protein, validating the editing approach. Clones highlighted in red were selected for further analyses.

2.2. FANCA-Mutant Clones Are Hypersensitive to ICL-Agents

The hypersensitivity to the chromosome-breaking effects of ICL-inducing agents provides a reliable cellular marker for the diagnosis of FA [17,18]. Cells from FA patients are extremely sensitive to such agents such as mitomycin C (MMC), a drug that is currently used as a diagnostic tool. Therefore, we tested the sensitivity of *FANCA*-mutant clones to MMC using cell viability assays, and the concentrations of MMC corresponding to its 50 inhibitory concentration (IC50) were calculated. IC50 values of mutant clones were 9.6 to 13.2 times lower than their corresponding parental cells, CAL27 and CAL33 (Figure 2A and Table 1). As expected, similar results were obtained with VU1365 cells, a FA patient–derived HNSCC cell line (*FANCA* mutated) previously described [11]. Defective VU1365 cells were 7.4 times more sensitive to MMC than *FANCA*-complemented cells (VU1365-FANCA) obtained upon retroviral transduction of a functional *FANCA* gene. Same findings were obtained with cisplatin, another ICL-inducing agent currently used as main chemotherapy in HNSCC (Figure 2B and Table 1).

To rule out that the drug sensitivity changes from parental cells to selected clones were due to clonal selection, we calculated IC50 values in CAL27-c27 and CAL33-c18 cells, which were nucleofected but non-edited (Figure S4). Results showed no differences in sensitivity to MMC (Table S3 and Figure S5). To confirm that MMC sensitivity in edited cells was due to the deficiency in FANCA and not associated to CRISPR-mediated off target effects, we complemented null cell lines with retroviral transduction of a functional *FANCA* gene and calculated sensitivity to MMC. Complemented cells displayed similar IC50 values than parental cells (Table S3 and Figure S5), therefore showing that differences in response upon ICL-inducing agents depends on *FANCA* mutations introduced during editing.
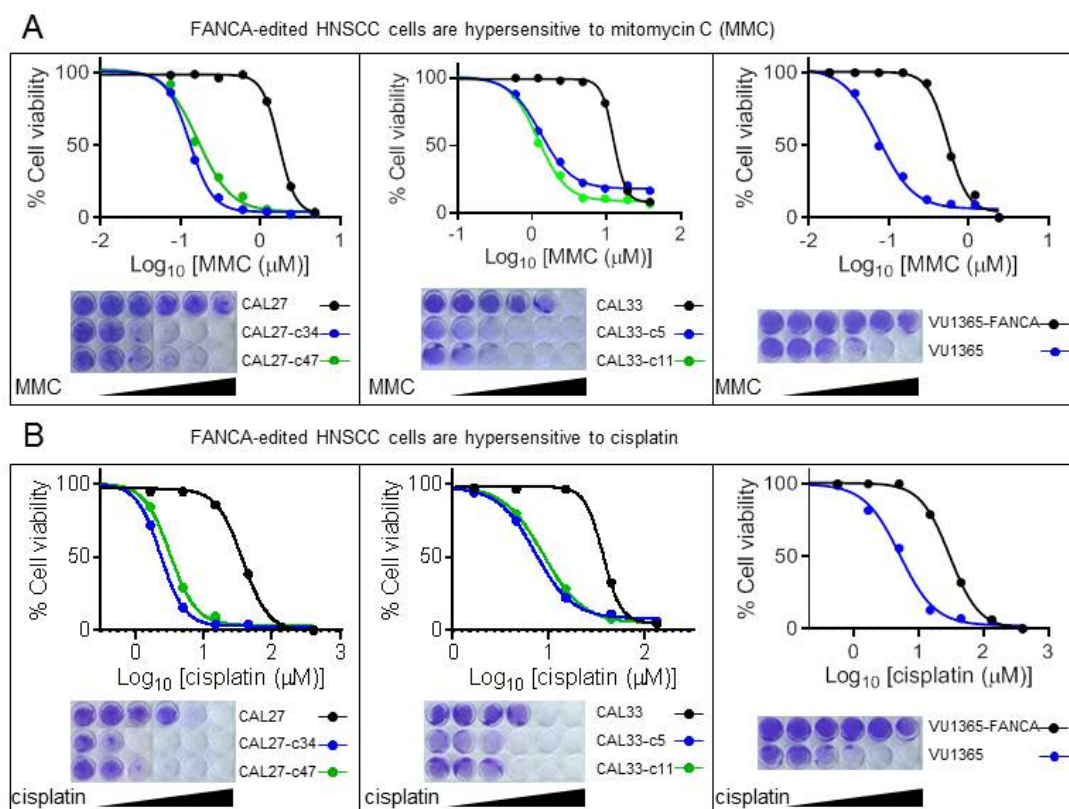

Figure 2. *FANCA*-edited HNSCC cells are hypersensitive to ICL agents. Cells were treated with increasing concentrations of mitomycin C (MMC) (**A**) or cisplatin (**B**) for 1 h and grown until control cells reached the maximum confluence (5 days). Cells were stained with crystal violet, eluted with acetic acid, and color intensity was measured with absorbance at 620 nm. Data represent means ± SEMs from three different experiments for each cell line. *FANCA*-mutant CAL27 and CAL33 edited clones are more sensitive than parental cells to MMC and cisplatin insults. As expected, VU1365 cancer cells from an FA patient are also more sensitive than *FANCA*-complemented, VU1365-FANCA cells.

Table 1. Half-maximal inhibitory concentration (IC50) values for mitomycin C (MMC) and cisplatin (microM).

Cell Line	IC50 MMC	Ratio Mutant/Non Mutant	IC50 Cisplatin	Ratio Mutant/Non Mutant
CAL27	1.704		37.560	
CAL27-c34	0.129	13.220	2.377	15.801
CAL27-c47	0.165	10.340	3.274	11.472
CAL33	12.490		37.130	
CAL33-c5	1.298	9.622	7.281	5.100
CAL33-c11	1.198	10.426	8.331	4.457
VU1365-FANCA	0.548		29.680	
VU1365	0.074	7.363	5.017	5.916

IC50 values are defined as the concentration of drug causing a decrease of 50% of cell viability upon clonogenic assays, cristal violet staining and quantification. Data are means from three different experiments for each cell line.

Overall, sensitivity assays demonstrated that engineered *FANCA* mutated clones from non-FA HNSCC cell lines are hypersensitive to ICL-agents.

2.3. FANCA-Mutant Clones Are Defective in FANCD2 Monoubiquitination and Nuclear Foci Formation

Early upon ICL, the FA core complex monoubiquitinates the FANCI-FANCD2 (ID2) complex, that accumulates in nuclear foci [19]. CAL27 and CAL33 cells were treated for 1 h at IC50 concentration of MMC. As expected, a protein band of higher molecular weight over FANCD2 protein was detected, representing the monoubiquitinated form of FANCD2 (Figure 3A). As reported, a similar result was obtained with VU1365-FANCA cells [20]. Moreover, immunofluorescence images showed that FANCD2 accumulated in nuclear foci of treated cells, corroborating that parental CAL27 and CAL33 cells have a functional FA pathway, as do the VU1365-FANCA cells (Figure 3B,C). Interestingly, CAL27-c34 and CAL33-c11 clones did not ubiquitinate FANCD2 (Figure 3A), and neither showed nuclear foci upon DNA damage (Figure 3B,C), suggesting a defective FA pathway similar to FA-HNSCC cells VU1365 (Figure 3B,C) [20] or blood cells and fibroblasts from FA patients.

2.4. Increased Chromosome Fragility and G2 Arrest in FANCA-Mutant Clones

Micronuclei (MN) are chromosome fragments that are left behind in anaphase and appear in daughter cells as small additional nuclei. MN formation is considered a surrogate marker of chromosomal fragility. Increased MN frequency has been found in buccal mucosa cells from patients with defects in DNA-repair pathways, and has been proposed as a biomarker of cancer risk in FA patients [21]. *FANCA*-mutant and parental CAL27 and CAL33 cells were treated with diepoxybutane (DEB) during 48 h and the MN frequency was measured. Results showed that mutant clones had increased MN frequency when compared with their corresponding parental cells (Figure 4A), consistent with exacerbated chromosome fragility. Moreover, mutant cells displayed increased G2 arrest after DEB treatment (Figure 4B), another hallmark of FA deficiency [22]. Both results support mutant clones as adequate models of FA-HNSCC disease.
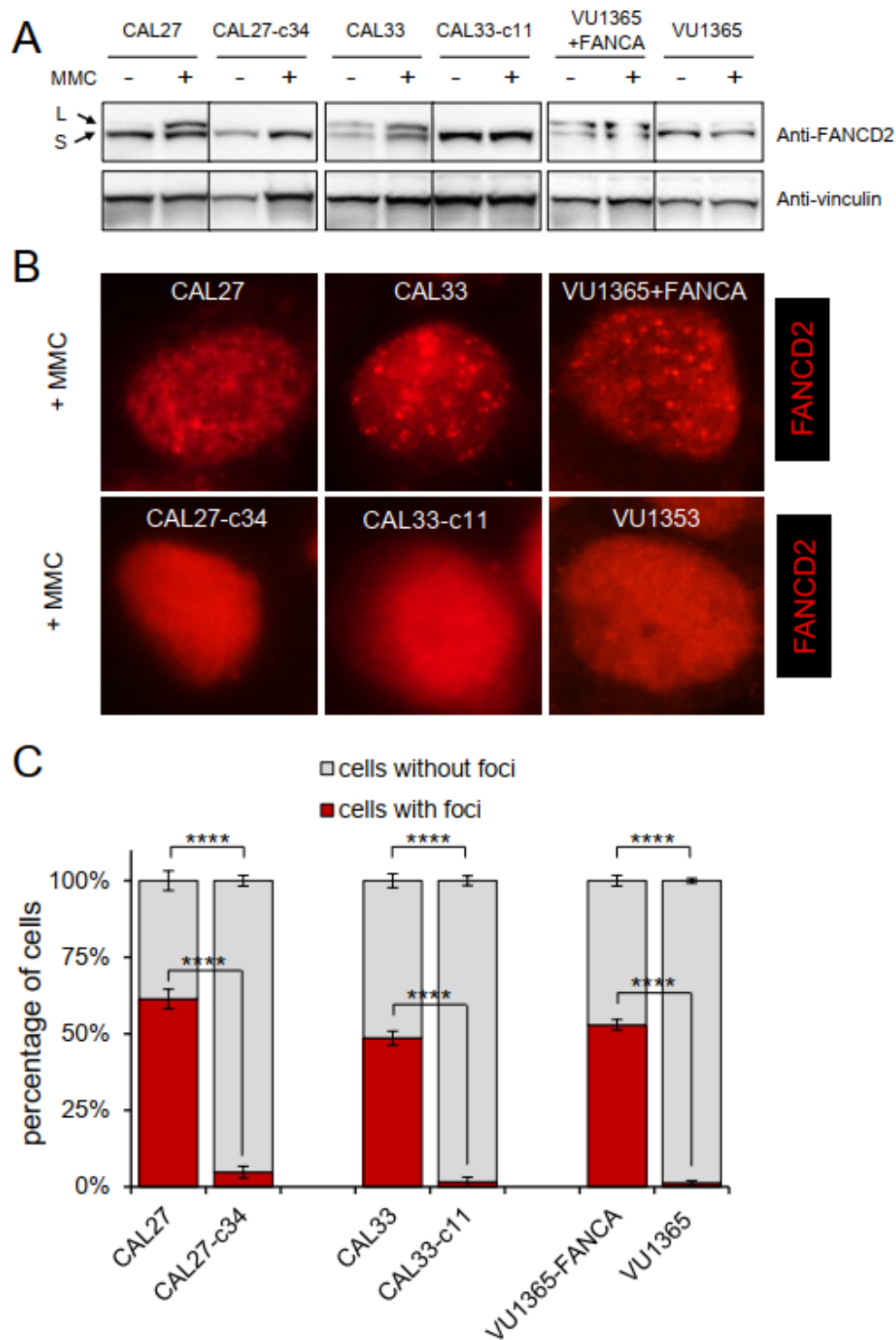
Figure 3. *FANCA*-edited HNSCC cells are defective in FANCD2 monoubiquitination and nuclear foci formation. CAL27, CAL33, and VU1365 parental and derivative cells were treated with IC50 concentration of MMC for 1 h and harvested. (**A**) Western blot with anti-FANCD2 antibody showing that FANCD2 monoubiquitination was not observed in *FANCA* mutant CAL27 and CAL33 clones (CAL27-c34 and CAL33-c11, respectively) suggesting a defective Fanconi pathway. As reported, parental VU1365 also lacked FANCD2 ubiquitination, which was corrected upon *FANCA* complementation (VU1365-FANCA). A vinculin antibody was used as housekeeping control. (**B**) Immunofluorescence analysis with FANCD2 antibody. *FANCA*-mutant cells (CAL27-c34, CAL33-c11) cannot form nuclear foci after 1 h of MMC treatment at IC50 concentration. (**C**) Quantification of nuclear foci in treated and untreated cells. Data represent mean ± SEM. *p*-values were calculated using a two-way ANOVA test, ****: *p*-value ≤ 0.0001.
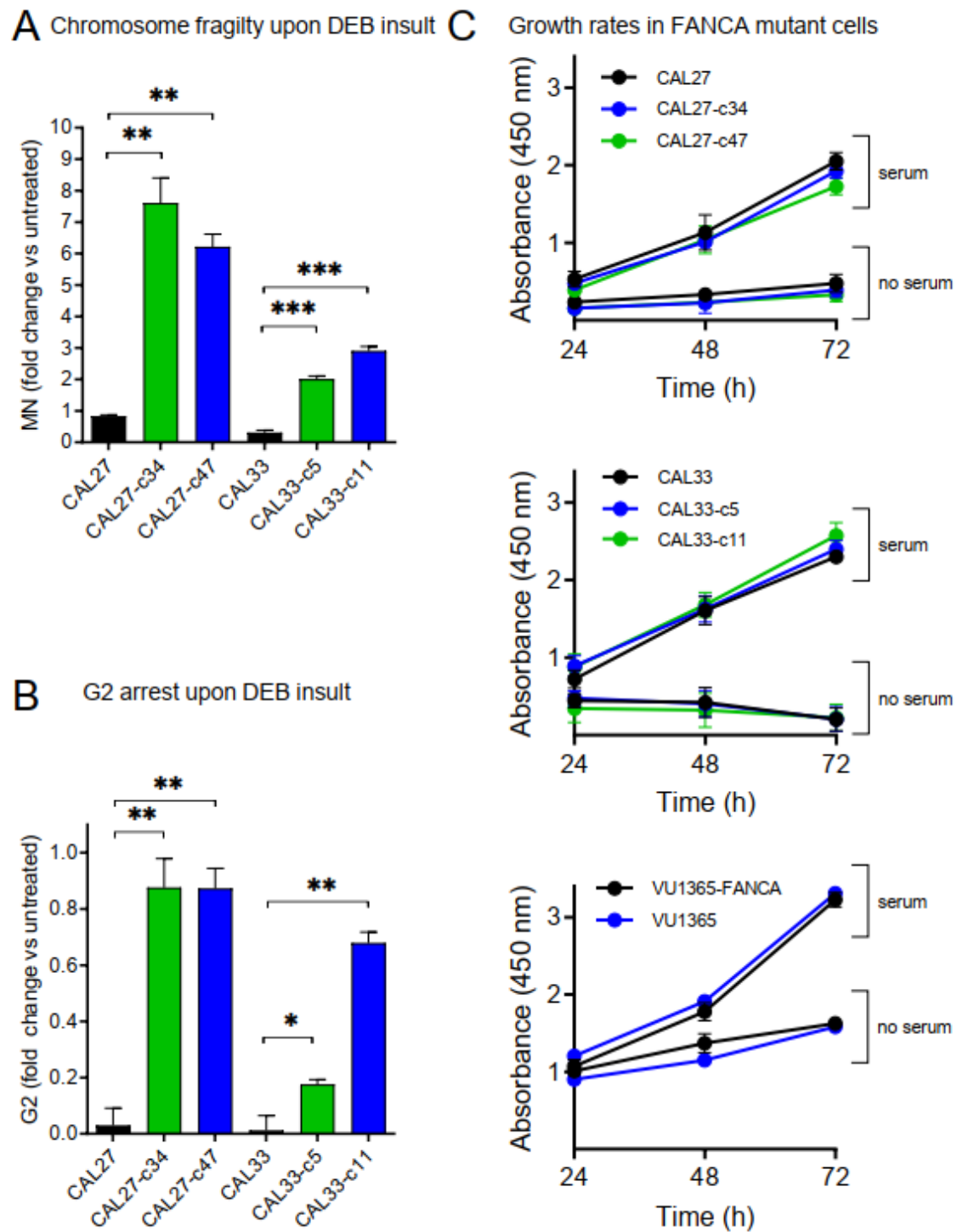
Figure 4. (**A**) Chromosome fragility analyzed by the micronucleus (MN) test. Cells were treated with diepoxybutane (DEB), kept in culture at for least one population doubling, and MN were quantified with flow cytometry. *FANCA*-edited clones displayed increased MN formation and therefore chromosome fragility. Data are means $\pm$ SEMs from three independent experiments, each one in duplicate. (**B**) Cells in G2 phase of the cell cycle were quantified upon DEB insult. *FANCA*-edited clones arrested in G2, as expected for dysfunctional FA pathway. Data are means $\pm$ SEMs from three independent experiments, each one in duplicate. (**C**) HNSCC cells were seeded and maintained in culture with (serum) or without (no serum) 10% FBS for 24, 48, and 72 h. Cell viability was measured using XTT assay and absorbance at 450 nm. *FANCA* mutation does not affect growth rate in HNSCC cells. *p*-values were calculated upon a T-Student test for independent samples (**A**,**B**) or upon a two-way ANOVA test (**C**). *: *p*-value$\leq$ 0.05; **: *p*-value$\leq$ 0.01; ***: *p*-value$\leq$ 0.001.

2.5. FANCA-Mutation Does Not Affect Growth Rates in HNSCC Cells

FA genes can affect cellular growth as their function is to assure DNA integrity. Transduction with therapeutic lentiviral vectors allow proliferative advantage of corrected versus *FANCA* mutant hematopoietic cells [23]. Additionally, adult Fanconi mice (Fanca$^{-/-}$ and Fancg$^{-/-}$) have reduced proliferation of neural progenitor cells [24]. We tested whether HNSCC cells with *FANCA*-mutation proliferate differently, both in standard (10%) or in non-serum conditions. Strikingly, results showed no differences between mutant clones and parental CAL27 and CAL33 cells, or between VU1365 and complemented VU1365-FANCA cells (Figure 4C). Therefore, a functional *FANCA* gene does not provide proliferative advantage on HNSCC cell lines.

2.6. FANCA-Mutation Augments Cell Migration in HNSCC Cells

FA patients with HNSCC have poorer clinical outcomes than non-FA patients, probably due to fewer treatment options. However, we cannot discard that FA deficiency might accelerate cancer progression by molecular mechanisms not fully understood. Increased in vitro migration/invasion was reported for sporadic HNSCC cell lines whereby FA genes were knocked-down with shRNA [25]. We evaluated migration capacity using scratch wound healing assays in CAL27/CAL33 mutant clones and VU1365 cells. Wound closure was measured for a period of 72 h, showing that HNSCC cells with *FANCA* mutation migrate faster and close the wound earlier (Figure 5). This result suggests that HNSCC with defective FA pathway might be more aggressive.
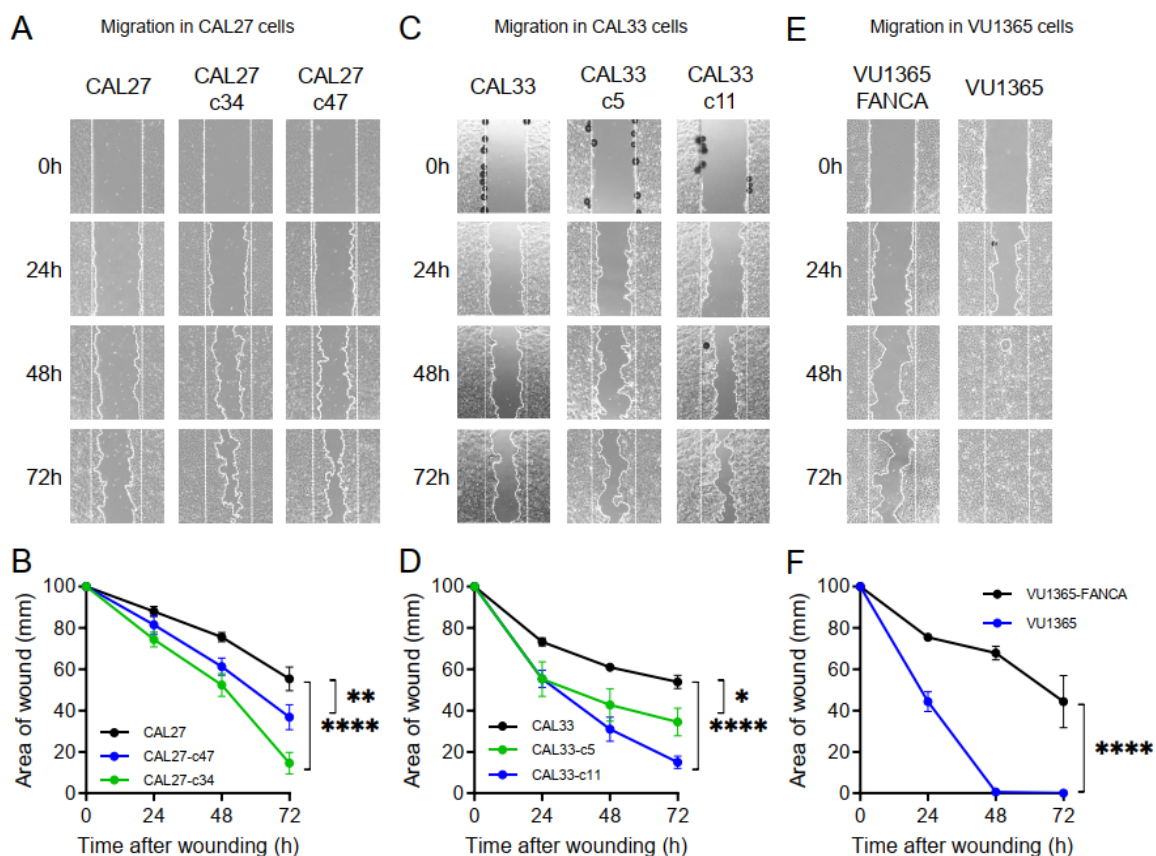

Figure 5. Migration analysis of *FANCA*-edited cells. (**A**,**C**,**E**): Representative images of keratinocyte sheets that were scratch wounded to assess migration. Scale bar: 100 μm. (**B**,**D**,**F**): Wound area analyzed at different times after wounding at 1% FBS. Data are mean ± SEM of one experiment with four images per time-point. *p*-values were calculated upon a two-way ANOVA test. *: *p*-value ≤ 0.05; **: *p*-value ≤ 0.01; ****: *p*-value ≤ 0.0001. CAL27 and CAL33 edited clones as well as VU1365 cells migrated faster as they closed the wounds earlier.

Overall, our CRISPR/Cas9 strategy to obtain *FANCA*-mutant clones from non-FA HNSCC cell lines gave adequate FA-HNSCC disease models as mutant clones, which (i) are hypersensitive to ICL-agents MMC and cisplatin, (ii) cannot monoubiquitinate FANCD2 and form nuclear foci upon MMC treatment, and (iii) display increased chromosome fragility and G2 arrest when treated with DEB. Importantly, mutant cells migrate faster and constitute a useful tool to investigate molecular and cellular mechanisms linking the FA pathway with invasive phenotypes.

3. Discussion

A few HNSCC cell lines from FA patients exist, including VU1365, which we use here. Increasing the number of cell lines and incorporating those with classical HNSCC mutations are necessary to find adequate new treatments for FA patients with HNSCC. Such treatments should not induce chromosome fragility to avoid toxicities that might preclude their clinical use. Therefore, we predict that our *FANCA*-mutant clones from CAL27 and CAL33 will be useful in this context.

CAL27 and CAL33 are well studied cell lines that have known aberrations/mutations in classical HNSCC genes such as *TP53* (CAL27/CAL33), *PIK3CA* (CAL33), *FAT1* (CAL27/CAL33), *CASP8* (CAL33), etc. [13]. Oncogenic signaling and response to cetuximab, cisplatin, and radiotherapy has been thoughtfully investigated in these cell lines [26–28]. In addition, sensitivity profiles for many compounds and their association with molecular aberrations have been determined for CAL27 and CAL33 as part of the cell lines within consortiums such as CCLE [14], Genomics of Drug Sensitivity in Cancer [29], and Cancer Dependency Map (https://depmap.org/portal/depmap/, accessed on 1 November 2020). Therefore, links between distinct pharmacologic vulnerabilities to genomic patterns and translation into cancer patient stratification is possible for CAL27 and CAL33 [12]. How some of these vulnerabilities change upon *FANCA* mutation should be investigated in the future.

The CRISPR/Cas9 strategy that we use results in very high editing frequencies (>90%, see Figure 1). Possible factors include the absence of a functional p53 pathway in CAL27 and CAL33, which has been shown to inhibit CRISPR/Cas9 editing. Also, given that mutating *FANCA* in these cells did not reduce growth rates (Figure 4C), no negative selection of mutant versus non-mutant clones soon after nucleofection occurs. We predict that other gene editing attempts in additional FA genes should also be feasible in this setting.

CAL27 and CAL33 cell lines monoubiquitinate FANCD2 and form FANCD2 nuclear foci after ICL damage, demonstrating a functional FA pathway (Figure 3). Such activities were impeded upon biallelic inactivating *FANCA* mutations in cell clones obtained after CRISPR/Cas9 editing which also make cells hypersensitive to MMC and cisplatin (Figure 2). Furthermore, *FANCA*-mutated clones from CAL27 and CAL33 treated with DEB displayed chromosome fragility and G2 arrest (Figure 3A,B). All these findings clearly demonstrated that CAL27-c34 and -c47 clones, and CAL33-c5 and -c11 clones have defective FA pathway, and therefore, they constitute new FA-HNSCC cellular models.

A functional *FANCA* gene does not provide proliferative advantage to CAL27, CAL33, or VU1365-FANCA cells (Figure 3C) in cell culture. A similar result was reported for VU1365 parental and *FANCA*-complemented cells grown in three-dimensional cultures [20]. These results are in contrast with the reduced viability of FA-deficient hematopoietic cells. Although a synchrony between FA gene expression and the cell cycle in HNSCC cell lines has been shown [30], further analysis might help to understand whether the FA pathway can have role in the proliferative potential in HNSCC.

Response to current therapies of FA patients with HNSCC is very poor, partially due to toxicities to chemo/radio therapies. Moreover, most patients are diagnosed in advanced stages and recurrent/metastatic disease is frequent. However, we cannot rule out an involvement of the FA pathway in tumor progression. We have found that *FANCA* mutant HNSCC cells, either from FA or non-FA patients, display increased in vitro migration speed when compared with FA pathway proficient counterparts (Figure 5). This result is in line

with reports indicating that HNSCC with DNA repair defects display features of invasive disease [31–33]. More specifically, increased in vitro invasiveness of sporadic HNSCC cell lines where FA genes have been knocked-down with shRNA was also reported [25]. We propose that *FANCA*-mutant clones from CAL27 and CAL33 are good tools to deepen into molecular mechanisms of tumor progression mediated by FA genes.

HNSCC is a life-threating health complication in FA patients for whom standard therapies are poorly effective. New FA-HNSCC disease models are needed to understand the molecular mechanisms of disease progression, eventually leading to the discovery of druggable targets to develop new therapies. Here, we describe new cell lines obtained from individual clones of edited CAL27 and CAL33 cells which faithfully phenocopy defective FA pathway, and can be stably grown in standard cultured conditions. We propose these clones as FA-HNSCC disease models that might help to find new therapies.

4. Materials and Methods

4.1. Cell Culture and Genotoxic Agents

Tongue SCC cell lines CAL33 and CAL27 were provided by Dr. Silvio Gutkind (UC San Diego, CA, USA). VU1365, a mouth mucosa SCC cell line from a FA patient, was provided by Dr. Josephine Dorsman (Amsterdam UMC, Holland). Clones 34 and 47 from CAL27 (CAL27-c34 and CAL27-c47) and clones 5 and 11 from CAL33 (CAL33-c5 and CAL33-c11) were obtained using CRISPR/Cas9 editing (see below). *FANCA* complemented VU1365-FANCA, CAL27-c34-FANCA, CAL27-c47-FANCA, CAL33-c5-FANCA, and CAL33-c11-FANCA cells were made from VU1365, CAL27-c34, CAL27-c47, CAL33-c5, and CAL33-c11, respectively, upon two rounds of transduction with a retroviral vector carrying the cDNAs for *FANCA* and the neomycin resistance gene (S11FAIN) [34]. Then, 48 h after transduction, cells were selected with G418 at 0.7mg/mL (Calbiochem, Merck, Darmstadt, Germany) for five days and expanded prior to use. All parental and derivative cells were cultured in Dulbecco's Modified Eagle's Medium (DMEM) (Gibco, Thermo Fisher Scientific, Waltham, MA, USA) supplemented with 10% fetal bovine serum (FBS) (Gibco, Thermo Fisher Scientific) and maintained at 37 °C, in an atmosphere of 5% CO_2 and 95% humidity. CAL27 and CAL33 parental and cloned cells were authenticated using short tandem repeat (STR) profiling.

4.2. Cell Line Nucleofection and CRISPR/Cas9 Editing within Exon 4 of FANCA Gene

CRISPR/Cas9 genome editing was performed by ribonucleotide-protein (RNP) nucleofection using the 4D-Nucleofector™ System (Lonza, Basel, Switzerland), following the electroporation conditions already optimized in the laboratory, which included the use of 15-EW program and the SE Solution (Lonza). Thus, Streptococcus pyogenes Cas9 nuclease (IDT), together with a chemically modified, stable synthetic guide RNA (crRNA) specific for exon 4 of *FANCA* gene linked to tracrRNA (gGM10) (Synthego) were used (Figure S2A). The range of concentrations used was between 0.5–3 μg for Cas9 and 0.7–4 μg for gGM10 guide. Cell viability was analyzed 24 h later using flow cytometry (BD LSR-FortessaTM, BD Biosciences) and DAPI (Roche, Basel, Switzerland) labeling, and data analyzed with FlowJo. Exon 4 from *FANCA* gene was subsequently amplified by PCR, using specific primers (Table S2) and the Herculase II fusion DNA polymerase (Agilent, Santa Clara, CA, USA). Previous to that, DNA was purified with the DNeasy Blood & Tissue (Qiagen, Hilden, Germany). Editing efficiency was evaluated via nuclease assay using the corresponding Surveyor® Mutation Detection Kit (IDT). DNA fragments resulting from nuclease activity during the Surveyor assay were separated by electrophoresis in 10% TBE-polyacrylamide gels (Thermo Fisher Scientific). A quantitative measurement of optical density through Image J was performed to quantify efficiency of CRISPR/Cas9 editing. Optical density (OD) intensity was calculated from both edited DNA bands (ed1 and ed2) and non-edited bands (non-ed) applying the following formula: % edition = [(DO_ed1+ DO_ed2 − 2 × DO_background)/(DO_non_ed+DO_ed1+DO_ed2 − 3 × DO_background)] × 100. Once nucleofection was performed, individual cell clones were

seeded separately in 96-well plates using cell sorting (Influx BD^{TM}) and amplified with conditioned medium. *FANCA* gene locus was then PCR amplified and sequenced from genomic DNA of selected clones through the Sanger method (StabVida, Caparica, Portugal), using the primer P_GM_Forward4 (Table S2). Afterwards, ICE CRISPR Software Analysis Tool (Synthego, Redwood City, CA, USA) was used to quantify and analyze editing results.

4.3. Protein Extraction and Western Blotting

Protein extracts were obtained using a lysis buffer (Hepes 40 mM, Triton-X100 2%, β-glycerophosphate 80 mM, NaCl 200 mM, MgCl$_2$ 40 mM, EGTA 20 mM) supplemented with protease and phosphatase inhibitor cocktails (Roche). Proteins were separated in 4–12% Nu-Page Bis-Tris (FANCA analysis) or NuPAGE 3–8% Tris-Acetate (FANCD2) polyacrylamide gels (Invitrogen) and transferred to nitrocellulose membranes (Amersham Biotech) under wet conditions. Membranes were blocked with 5% non-fat milk in TBS-Tween (Tris-HCl 20 mM, NaCl 137 mM, Tween-20 0.5%) and incubated with the primary antibodies anti-FANCA (1:1000, Abcam), anti-FANCD2 (1:200, Santa Cruz Biotechnology, Dallas, TX, USA), anti-vinculin (Abcam, Cambridge, UK), and anti-GAPDH (1:5000, Santa Cruz, Dallas, TX, USA). Peroxidase-coupled, secondary antibodies specific for rabbit IgG (1:5000, Amersham, Little Chalfont, UK) and mouse IgG (1:5000, Jackson, West Grove, PA, United States) were also used. Bands were visualized with the luminescence detection kit Super Signal West Pico Chemiluminscence Substrate (Pierce, Thermo Fisher Scientific, Waltham, MA, USA) according to manufacturer's instructions, and quantified using the Image Lab 5.2.1 software (BioRad, Hercules, CA, USA). GAPDH and vinculin proteins were selected as loading controls.

4.4. Mitomycin C (MMC) and Cisplatin Sensitivity Assays

To test the MMC and cisplatin-induced cytotoxicity, clonogenic assays on SCC cells were performed. Thus, 40,000 cells from CAL27, CAL27-c27, CAL27-c34, CAL27-c34-FANCA, CAL27-c47, CAL27-c47-FANCA, VU1365, and VU1365-FANCA, and 100,000 cells from CAL33, CAL33-c18, CAL33-c5, CAL33-c5-FANCA, CAL33-c11, and CAL33-c11-FANCA were seeded on 6-well plates and 24 h later treated with a range of MMC or cisplatin concentrations for 1 h. Afterwards, cells were washed three times with PBS and cultured in DMEM until control cells reached the maximum confluence (5 days). Finally, cells were stained with crystal violet and eluted with 33% acetic acid. Color intensity was measured using the Genius Pro (Tecan, Männedorf, Switzerland) microplate reader (absorbance at 620 nm). Each experiment was carried out at least three times. The concentrations of MMC and cisplatin corresponding to its 50 inhibitory concentration (IC50) were calculated.

4.5. FANCD2 Immunofluorescence

For the FANCD2 immunofluorescence, 40,000 cells from CAL27, CAL27-c34, VU1365, and VU1365-FANCA, or 100,000 cells from CAL33, CAL33-c11 were cultured on 2-well coverslips (Chamber cell culture slides, FALCON) and treated with IC50 concentration values of mitomycin C (MMC) for 1 h. Subsequently, cells were fixed with 4% formaldehyde for 15 min, permeabilized with 0.5%-Triton-X100 for 5 min and blocked with 0.1%-NP-40 FBS (Sigma-Aldrich, St. Louis, MO, USA) for 1 h, to avoid non-specific binding. Thereafter, cells were incubated with the primary antibody anti-FANCD2 (1:200, Abcam) at 4 °C for 12 h. Fluorochrome-complex rabbit IgG specific antibody AlexaFluor 594, (1:1000, Jackson) was used as a secondary antibody. Finally, mounting of slides was carried out using MOWIOL with DAPI (200 μg/mL) for nucleus detection. Visualization was performed using Axioplan 2 imaging (Zeiss, Oberkochen, Germany) microscope, and images were captured with AxioCam MRm (Zeiss) and visualized through the AxioVision Rel.4.6 (Zeiss) software.

4.6. Chromosome Fragility and G2 Arrest by the Flow Cytometry Micronucleus (MN) Test

Cells were processed by flow cytometry following the procedure previously described by Avlasevich et al. [35] and reported with some modifications by Hernandez et al. [36]. Briefly, 10,000 cells from each cell line were seeded in 96-well plates. The next day cultures were untreated or treated with 0.05 µg/mL of diepoxybutane (DEB) and kept in culture for at least one population doubling. Cells were then sequentially stained: first with ethidium monoazyde bromide (EMA) (0.025 mg/mL) and, secondly, in lysis solution, with 4′,6-diamidino-2-phenylindole (DAPI) (2 µg/mL). After that, samples were stored at 4 °C until being processed in a MACSQuant Analyzer 10 cytometer (Miltenyi, Bergisch Gladbach, Germany). Collected data were analyzed by Flow Jo VX software. The data of micronuclei (MN) and G2 arrest presented in this work represent results from three independent experiments each one in duplicate.

4.7. Cell Growth Assays

Altogether, 2000 cells from CAL27, CAL27-c34, CAL27-c47, VU1365, and VU1365-FANCA, and 4000 cells from CAL33, CAL33-c5, and CAL33-c11 were seeded in 96-well plates and cell viability was determined with the colorimetric Cell Proliferation Kit II (XTT) (Roche) 24, 48, and 72 h later, following the manufacturer's instructions. Absorbance values were measured using the Genius Pro (Tecan) microplate reader. Each experiment was performed at least three times, with six replicates of each cell line for the assay. Background absorbance was subtracted, and data were normalized to the corresponding values of 24-h measurement. Cells were maintained either in 10% FBS or 0% FBS.

4.8. Wound Healing Assay for Cell Migration Analysis

Cell migration was analyzed using the in vitro wound healing method. Briefly, 400,000 cells from CAL27, CAL27-c34, VU1365, and VU1365-FANCA, or 600,000 cells from CAL33 and CAL33-c11 were seeded in 6-well plates and 24 h later the FBS concentration was reduced to 1% in order to stop cell proliferation. Cells were maintained under these conditions for 72 h, and, after this time, two straight lines were scratched within each plate, creating wounds of approximately 1 mm. Wound closure area was calculated 0, 24, 48, and 72 h later. Gap distances were quantitatively measured using Image J software. Wound area quantification data are mean ± SEM of three different wounds of three independent experiments.

4.9. Statistical Analysis

The half maximal inhibitory concentration (IC50) values are defined as the drug concentrations required for 50% loss of cell viability in a clonogenic assay, using a non-linear regression fit. Data are shown as mean ± standard error of the mean (SEM). For cell proliferation and cell migration assays, one-way ANOVA or two-way ANOVA were done respectively. A p-value > 0.05 (ns), ≤ 0.05 (*), ≤ 0.01 (**), ≤ 0.001 (***), ≤ 0.0001 (****) was considered. Graphs and statistics were done using GraphPad Prism 8 software.

Supplementary Materials: The following are available online at https://www.mdpi.com/article/10.3390/genes12040548/s1, Figure S1: Expression values of *FANCA* gene mRNA from The Cancer Cell Line Encyclopedia collection, Figure S2: Edited sequences in CAL27 mutant clones. Figure S3: Edited sequences in CAL33 mutant clones. Figure S4: Non-edited sequences in CAL27 and CAL33 wild type clones. Figure S5: Sensitivity to MMC in non-edited, edited and *FANCA*-complemented clones. Table S1: Gene expression values and copy-number status of the *FANCA* gene in the Cancer Cell Line Enciclopedia (CCLE) collection. Table S2: Primers used for nuclease assay and Sanger sequencing after *FANCA* gene editing. Table S3: IC50 values for MMC in parental, non-edited, edited, and *FANCA*-complemented clones from CAL27 and CAL33.

References

1. Bogliolo, M.; Surralles, J. Fanconi anemia: A model disease for studies on human genetics and advanced therapeutics. *Curr. Opin. Genet. Dev.* **2015**, *33*, 32–40. [CrossRef] [PubMed]
2. Niraj, J.; Farkkila, A.; D'andrea, A.D. The Fanconi Anemia Pathway in Cancer. *Annu. Rev. Cancer Biol.* **2019**, *3*, 457–478. [CrossRef] [PubMed]
3. Rio, P.; Navarro, S.; Wang, W.; Sanchez-Dominguez, R.; Pujol, R.M.; Segovia, J.C.; Bogliolo, M.; Merino, E.; Wu, N.; Salgado, R.; et al. Successful engraftment of gene-corrected hematopoietic stem cells in non-conditioned patients with Fanconi anemia. *Nat. Med.* **2019**, *25*, 1396–1401. [CrossRef]
4. Risitano, A.M.; Marotta, S.; Calzone, R.; Grimaldi, F.; Zatterale, A.; Contributors, R. Twenty years of the Italian Fanconi Anemia Registry: Where we stand and what remains to be learned. *Haematologica* **2016**, *101*, 319–327. [CrossRef] [PubMed]
5. Alter, B.P.; Giri, N.; Savage, S.A.; Rosenberg, P.S. Cancer in the National Cancer Institute inherited bone marrow failure syndrome cohort after fifteen years of follow-up. *Haematologica* **2018**, *103*, 30–39. [CrossRef] [PubMed]
6. Li, J.; Sipple, J.; Maynard, S.; Mehta, P.A.; Rose, S.R.; Davies, S.M.; Pang, Q. Fanconi anemia links reactive oxygen species to insulin resistance and obesity. *Antioxid. Redox. Signal.* **2012**, *17*, 1083–1098. [CrossRef]
7. Zhang, Q.S.; Tang, W.; Deater, M.; Phan, N.; Marcogliese, A.N.; Li, H.; Al-Dhalimy, M.; Major, A.; Olson, S.; Monnat, R.J., Jr.; et al. Metformin improves defective hematopoiesis and delays tumor formation in Fanconi anemia mice. *Blood* **2016**, *128*, 2774–2784. [CrossRef]
8. Kutler, D.I.; Patel, K.R.; Auerbach, A.D.; Kennedy, J.; Lach, F.P.; Sanborn, E.; Cohen, M.A.; Kuhel, W.I.; Smogorzewska, A. Natural history and management of Fanconi anemia patients with head and neck cancer: A 10-year follow-up. *Laryngoscope* **2016**, *126*, 870–879. [CrossRef]
9. Montanuy, H.; Martinez-Barriocanal, A.; Casado, J.A.; Rovirosa, L.; Ramirez, M.J.; Nieto, R.; Carrascoso-Rubio, C.; Riera, P.; Gonzalez, A.; Lerma, E.; et al. Gefitinib and afatinib show potential efficacy for Fanconi anemia-related head and neck cancer. *Clin. Cancer Res.* **2020**, *26*, 3044–3057. [CrossRef]
10. Van Harten, A.M.; Poell, J.B.; Buijze, M.; Brink, A.; Wells, S.I.; Rene Leemans, C.; Wolthuis, R.M.F.; Brakenhoff, R.H. Characterization of a head and neck cancer-derived cell line panel confirms the distinct TP53-proficient copy number-silent subclass. *Oral Oncol.* **2019**, *98*, 53–61. [CrossRef]
11. Van Zeeburg, H.J.; Snijders, P.J.; Pals, G.; Hermsen, M.A.; Rooimans, M.A.; Bagby, G.; Soulier, J.; Gluckman, E.; Wennerberg, J.; Leemans, C.R.; et al. Generation and molecular characterization of head and neck squamous cell lines of fanconi anemia patients. *Cancer Res.* **2005**, *65*, 1271–1276. [CrossRef] [PubMed]
12. Ghandi, M.; Huang, F.W.; Jane-Valbuena, J.; Kryukov, G.V.; Lo, C.C.; Mcdonald, E.R.; 3rd Barretina, J.; Gelfand, E.T.; Bielski, C.M.; Li, H.; et al. Next-generation characterization of the Cancer Cell Line Encyclopedia. *Nature* **2019**, *569*, 503–508. [CrossRef] [PubMed]
13. Martin, D.; Abba, M.C.; Molinolo, A.A.; Vitale-Cross, L.; Wang, Z.; Zaida, M.; Delic, N.C.; Samuels, Y.; Lyons, J.G.; Gutkind, J.S. The head and neck cancer cell oncogenome: A platform for the development of precision molecular therapies. *Oncotarget* **2014**, *5*, 8906–8923. [CrossRef] [PubMed]

14. Barretina, J.; Caponigro, G.; Stransky, N.; Venkatesan, K.; Margolin, A.A.; Kim, S.; Wilson, C.J.; Lehar, J.; Kryukov, G.V.; Sonkin, D.; et al. The Cancer Cell Line Encyclopedia enables predictive modelling of anticancer drug sensitivity. *Nature* **2012**, *483*, 603–607. [CrossRef]

15. Palacios-Garcia, J.; Sanz-Flores, M.; Asensio, A.; Alvarado, R.; Rojo-Berciano, S.; Stamatakis, K.; Paramio, J.M.; Cano, A.; Nieto, M.A.; Garcia-Escudero, R.; et al. G-protein-coupled receptor kinase 2 safeguards epithelial phenotype in head and neck squamous cell carcinomas. *Int. J. Cancer* **2019**, *147*, 218–229. [CrossRef]

16. Hsiau, T.; Conant, D.; Rossi, N.; Maures, T.; Waite, K.; Yang, J.; Joshi, S.; Kelso, R.; Holden, K.; Enzmann, B.L.; et al. Inference of CRISPR Edits from Sanger Trace Data. *bioRxiv* **2019**. [CrossRef]

17. Giampietro, P.F.; Adler-Brecher, B.; Verlander, P.C.; Pavlakis, S.G.; Davis, J.G.; Auerbach, A.D. The need for more accurate and timely diagnosis in Fanconi anemia: A report from the International Fanconi Anemia Registry. *Pediatrics* **1993**, *91*, 1116–1120.

18. Auerbach, A.D. Fanconi anemia diagnosis and the diepoxybutane (DEB) test. *Exp. Hematol.* **1993**, *21*, 731–733.

19. Garcia-Higuera, I.; Taniguchi, T.; Ganesan, S.; Meyn, M.S.; Timmers, C.; Hejna, J.; Grompe, M.; D'andrea, A.D. Interaction of the Fanconi anemia proteins and BRCA1 in a common pathway. *Mol. Cell.* **2001**, *7*, 249–262. [CrossRef]

20. Lombardi, A.J.; Hoskins, E.E.; Foglesong, G.D.; Wikenheiser-Brokamp, K.A.; Wiesmuller, L.; Hanenberg, H.; Andreassen, P.R.; Jacobs, A.J.; Olson, S.B.; Keeble, W.W.; et al. Acquisition of Relative Interstrand Crosslinker Resistance and PARP Inhibitor Sensitivity in Fanconi Anemia Head and Neck Cancers. *Clin. Cancer Res.* **2015**, *21*, 1962–1972. [CrossRef]

21. Ramirez, M.J.; Minguillon, J.; Loveless, S.; Lake, K.; Carrasco, E.; Stjepanovic, N.; Balmana, J.; Catala, A.; Mehta, P.A.; Surralles, J. Chromosome fragility in the buccal epithelium in patients with Fanconi anemia. *Cancer Lett.* **2020**, *472*, 1–7. [CrossRef]

22. Chandra, S.; Levran, O.; Jurickova, I.; Maas, C.; Kapur, R.; Schindler, D.; Henry, R.; Milton, K.; Batish, S.D.; Cancelas, J.A.; et al. A rapid method for retrovirus-mediated identification of complementation groups in Fanconi anemia patients. *Mol. Ther.* **2005**, *12*, 976–984. [CrossRef]

23. Rio, P.; Navarro, S.; Guenechea, G.; Sanchez-Dominguez, R.; Lamana, M.L.; Yanez, R.; Casado, J.A.; Mehta, P.A.; Pujol, M.R.; Surralles, J.; et al. Engraftment and in vivo proliferation advantage of gene-corrected mobilized CD34(+) cells from Fanconi anemia patients. *Blood* **2017**, *130*, 1535–1542. [CrossRef]

24. Sii-Felice, K.; Etienne, O.; Hoffschir, F.; Mathieu, C.; Riou, L.; Barroca, V.; Haton, C.; Arwert, F.; Fouchet, P.; Boussin, F.D.; et al. Fanconi DNA repair pathway is required for survival and long-term maintenance of neural progenitors. *EMBO J.* **2008**, *27*, 770–781. [CrossRef]

25. Romick-Rosendale, L.E.; Hoskins, E.E.; Privette Vinnedge, L.M.; Foglesong, G.D.; Brusadelli, M.G.; Potter, S.S.; Komurov, K.; Brugmann, S.A.; Lambert, P.F.; Kimple, R.J.; et al. Defects in the Fanconi Anemia Pathway in Head and Neck Cancer Cells Stimulate Tumor Cell Invasion through DNA-PK and Rac1 Signaling. *Clin. Cancer Res.* **2016**, *22*, 2062–2073. [CrossRef]

26. Wang, Z.; Martin, D.; Molinolo, A.A.; Patel, V.; Iglesias-Bartolome, R.; Degese, M.S.; Vitale-Cross, L.; Chen, Q.; Gutkind, J.S. mTOR co-targeting in cetuximab resistance in head and neck cancers harboring PIK3CA and RAS mutations. *J. Natl. Cancer Inst.* **2014**, *106*. [CrossRef] [PubMed]

27. Huang, K.K.; Jang, K.W.; Kim, S.; Kim, H.S.; Kim, S.M.; Kwon, H.J.; Kim, H.R.; Yun, H.J.; Ahn, M.J.; Park, K.U.; et al. Exome sequencing reveals recurrent REV3L mutations in cisplatin-resistant squamous cell carcinoma of head and neck. *Sci. Rep.* **2016**, *6*, 19552. [CrossRef] [PubMed]

28. Eke, I.; Deuse, Y.; Hehlgans, S.; Gurtner, K.; Krause, M.; Baumann, M.; Shevchenko, A.; Sandfort, V.; Cordes, N. β1 Integrin/FAK/cortactin signaling is essential for human head and neck cancer resistance to radiotherapy. *J. Clin. Invest.* **2012**, *122*, 1529–1540. [CrossRef] [PubMed]

29. Garnett, M.J.; Edelman, E.J.; Heidorn, S.J.; Greenman, C.D.; Dastur, A.; Lau, K.W.; Greninger, P.; Thompson, I.R.; Luo, X.; Soares, J.; et al. Systematic identification of genomic markers of drug sensitivity in cancer cells. *Nature* **2012**, *483*, 570–575. [CrossRef] [PubMed]

30. Hoskins, E.E.; Gunawardena, R.W.; Habash, K.B.; Wise-Draper, T.M.; Jansen, M.; Knudsen, E.S.; Wells, S.I. Coordinate regulation of Fanconi anemia gene expression occurs through the Rb/E2F pathway. *Oncogene* **2008**, *27*, 4798–4808. [CrossRef]

31. Bakhoum, S.F.; Ngo, B.; Laughney, A.M.; Cavallo, J.-A.; Murphy, C.J.; Ly, P.; Shah, P.; Sriram, R.K.; Watkins, T.B.K.; Taunk, N.K.; et al. Chromosomal instability drives metastasis through a cytosolic DNA response. *Nature* **2018**, *553*, 467–472. [CrossRef] [PubMed]

32. Bhide, S.A.; Thway, K.; Lee, J.; Wong, K.; Clarke, P.; Newbold, K.L.; Nutting, C.M.; Harrington, K.J. Delayed DNA double-strand break repair following platin-based chemotherapy predicts treatment response in head and neck squamous cell carcinoma. *Br. J. Cancer* **2016**, *115*, 825–830. [CrossRef] [PubMed]

33. Essers, P.B.M.; Van Der Heijden, M.; Verhagen, C.V.M.; Ploeg, E.M.; De Roest, R.H.; Leemans, C.R.; Brakenhoff, R.H.; Van Den Brekel, M.W.M.; Bartelink, H.; Verheij, M.; et al. Drug Sensitivity Prediction Models Reveal a Link between DNA Repair Defects and Poor Prognosis in HNSCC. *Cancer Res.* **2019**, *79*, 5597–5611. [CrossRef]

34. Antonio Casado, J.; Callen, E.; Jacome, A.; Rio, P.; Castella, M.; Lobitz, S.; Ferro, T.; Munoz, A.; Sevilla, J.; Cantalejo, A.; et al. A comprehensive strategy for the subtyping of patients with Fanconi anaemia: Conclusions from the Spanish Fanconi Anemia Research Network. *J. Med. Genet.* **2007**, *44*, 241–249. [CrossRef] [PubMed]

35. Avlasevich, S.L.; Bryce, S.M.; Cairns, S.E.; Dertinger, S.D. In vitro micronucleus scoring by flow cytometry: Differential staining of micronuclei versus apoptotic and necrotic chromatin enhances assay reliability. *Environ. Mol. Mutagen.* **2006**, *47*, 56–66. [CrossRef]

36. Hernandez, G.; Ramirez, M.J.; Minguillon, J.; Quiles, P.; Ruiz De Garibay, G.; Aza-Carmona, M.; Bogliolo, M.; Pujol, R.; Prados-Carvajal, R.; Fernandez, J.; et al. Decapping protein EDC4 regulates DNA repair and phenocopies BRCA1. *Nat. Commun.* **2018**, *9*, 967. [CrossRef] [PubMed]